Electron Spin Resonance and Differential Scanning Calorimetry as Combined Tools for the Study of Liposomes in the Presence of Long Chain Nitroxides

Ilaria Perissi, Sandra Ristori, Simona Rossi, Luigi Dei, and Giacomo Martini*

Dipartimento di Chimica, Università di Firenze, Via della Lastruccia 3, 50019 Sesto Fiorentino, Firenze, Italy

Received: January 30, 2002; In Final Form: April 18, 2002

Macroscopic and molecular techniques such as differential scanning calorimetry (DSC) and electron spin resonance (ESR), respectively, were used to characterize both structure and dynamics of liposomes built up with dioleoyltrimethylammonium propane (DOTAP) and dioleoylphosphatidylethanolamine (DOPE) lipids. These liposomes are good candidates to act as molecular carriers in cancer therapy, such as, for instance, boron neutron capture therapy (BNCT). DSC revealed that neither T_m nor ΔH_m of the gel-liquid crystal phase transition depended on the presence of relatively concentrated exogenous molecules as they are the *n*-DSA and *n*-DPC spin probes used in this work. The results suggested that the structure and the internal dynamics of the liposomes did no change after small loading of the paramagnetic probes. This was proved at a molecular level by the computer analysis of the ESR spectra of the above probes, which revealed discontinuities of the motional parameters (correlation times, $\tau_\perp$ and $\tau_{||}$, and order parameter S_{20}) in the same range of temperatures of the endothermic events observed by DSC on probe-free liposomes. A dependence of $\tau_\perp$, $\tau_{||}$, and S_{20} on the localization of the probe was found, and the activation energies for the motion were consistent with the mobility of the domains sensed by the different probes. The results reported in this work may be considered as a useful basis for the characterization of both plain and loaded liposomes when these aggregates are used as drug carriers.

Introduction

Liposomes are typically spherical or quasispherical closed structures built up with one or more curved bilayers of amphiphilic molecules.[1−4] Because of their structural and dynamic features, they have been used as models for natural membranes able to entrap in their interior chemical species to which liposome bilayers are selectively permeable. In the last 30 years, liposomes have therefore been studied as potential drug carriers.[5] Since then, pharmacologically and biologically active molecules have been carried with opportunely tailored liposomes, and in the early 90s, the first commercial formulations for drug delivery were patented.[6]

In the past few years, some of the present authors studied the carrier properties of hydrocarbon/fluorocarbon vesicles, and they thoroughly characterized these mixed systems from a physicochemical point of view by means of magnetic resonance spectroscopies, scattering techniques, and Cryo-TEM, which allowed them to establish the perturbations induced by the presence of either molecules mimicking biological compounds or paramagnetic probes.[7−12]

In this work, the results obtained on cationic liposomes containing long chain nitroxides with a technique that gives mostly macroscopic information (differential scanning calorimetry, DSC) are compared with the results obtained with a technique that gives details mostly at a molecular level (electron spin resonance, ESR). The liposomes investigated were typical mixed liposomes formed with the neutral dioleoylphosphatidylethanolamine (DOPE) lipid and the cationic 1,2-dioleoyltrimethylammoniumpropane (DOTAP) lipid. These liposomes may be used as carriers for borocompounds in the boron neutron capture therapy (BNCT).[13]

Experimental Section

Materials. Aqueous dispersions of liposomes built up with DOPE (**1**, MW = 744.04) and DOTAP (**2**, MW = 698.55), in the 1:1 weight ratio, were purchased from Northern Lipids, Vancouver (Canada) or extruded directly from a mixture of the individual components with the Liposofast apparatus (Avestin Inc., Ottawa, Canada).

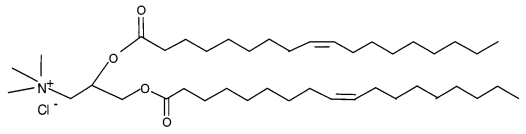

1

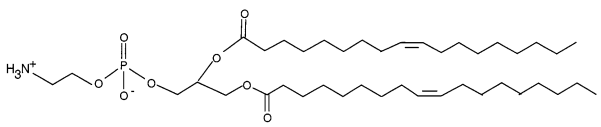

2

Total lipid content was10 mg/mL, pH = 6.5, and mean liposome diameter was 86 nm (data given by the manufacturer and checked by quasielastic light scattering). These dispersions were stored at 277 K. Their stability is given for at least 6 months.

* To whom correspondence should be addressed.

10.1021/jp0202845 CCC: $22.00
Published on Web 09/12/2002

Nitroxide radicals *n*-doxylphosphatidylcholine (*n*-DPC, **3**) and *n*-doxylstearic acid (*n*-DSA, **4**) were purchased from Sigma Chemicals, München, Germany, and used as received.

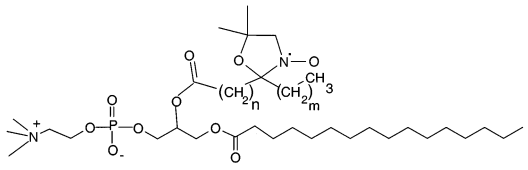

3

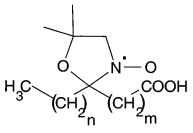

4

m = 3 *n* = 12 **3**: 5-DPC **4**: 5-DSA

m = 14 *n* = 1 **3**: 16-DSA **4**: 16-DSA

The surface per polar head is approximately 0.65 nm^2 for both DOTAP and DOPE.[14,15] On the basis of this value, samples were prepared with spin probe/liposome ratios in the range of 3500−7000 for DSC runs and 700−3500 for ESR runs.

Methods. DSC curves were obtained with the Perkin-Elmer DSC-7 calorimeter equipped with the TAC 7/DX interface and the software PE Pyris 3.52. Aluminum sealed containers were used for the measurements. Thermograms were recorded in the temperature range of 234−313 K with a scanning rate of 0.5 K/min. Data handling and treatment were as reported in ref 16.

ESR spectra were obtained with the aid of the Bruker model 200D spectrometer. Data acquisition was performed with the STELAR software. The temperature was controlled with Bruker VTB 3000 accessory. The accuracy was ±0.5 K. Quartz tubes of inner diameter <2 mm were used for ESR runs.

ESR data treatment was carried out by using the calculation procedure given by Freed and co-workers[17] and further developed by Budil et al.[18] which allows good simulation of the ESR spectra in very different motional conditions. In particular, the Brownian diffusion model for molecular reorientation was assumed in all cases, and the MOMD (microscopic order macroscopic disorder) model was applied when ESR probes were inserted in vesicles, as it is customarily done for this kind of systems.[19−21] In the Brownian reorientation model, the relationship between the correlation times $\tau_{\perp,\parallel}$ and the corresponding rotational diffusion rate constants $R_{\perp,\parallel}$ is the following:

$$\tau_{\perp,\parallel} = 1/6R_{\perp,\parallel}$$

The spin label microscopic orientational ordering was characterized here by the main term of the restoring potential as a function of the Wigner rotation matrix element ($kT\lambda D_{00}^2$) and by the corresponding order parameter $S_{20} = [\langle 3\cos^2\theta - 1\rangle]/2$, where θ is the angle between the nitroxide molecular axis and the normal to the bilayer. The macroscopic disorder of the system, caused by the random orientation of local bilayer directors, was taken into account by averaging spectra over 30 different orientations (NORT = 30). Sometimes, spin−spin effects such as Heisenberg spin−spin interactions in slow exchange conditions, affected ESR spectra, and they were also considered in the calculation.

Results and Discussion

The typical ESR three-line spectra of nitroxides are described in many papers, and simulation procedures are well established[22−25] for most of long-chain doxyl compounds in fluid solution when no aggregation occurs. This happened with *n*-DSA probes, **4**, at the concentration typically used in this work, whereas *n*-DPC nitroxides, **3**, formed aggregated in water at the same concentration (10^{-4} mol/dm^3 or higher). This was proven by the 310 K ESR spectrum of both 5- and 16-DPC recorded immediately after preparation of a relatively diluted water solution: for example, the spectrum of a 5×10^{-4} mol/dm^3 5-DPC water solution consisted in a very broad, single line. The measured line width ($\Delta B = 2.3$ mT) was consistent with the presence of aggregated structures, probably micelles. Spectra recorded after a few days showed a small contribution from a narrow triplet arising from nitroxide monomers in almost free motion conditions. The intensity of the triplet slowly increased with time. Hydrolysis of *n*-DPC to *n*-DSA could explain this effect.[25] The same was observed with 16-DPC. With *n*-DSA, no complication arose from spin−spin effects. The best fit magnetic parameters, which accurately reproduced most of the *n*-DSA and *n*-DPC spectra discussed in this paper, are reported in the Table 1.

TABLE 1: Best-Fit Magnetic Parameters Used to Reproduce the 310 K ESR Spectra of *n*-DPC and *n*-DSA in Water Solution[a] and after Insertion into DOTAP/DOPE Liposomes[b]

	g_{xx}	g_{yy}	g_{zz}	A_{xx}, G	A_{yy}, G	A_{zz}, G	$\tau_\perp$, sx10^{10}	n	S_{20}
Pure Water									
5-DSA	2.0080	2.0062	2.0029	6.2	5.8	35.4	1.9	2	
16-DSA	2.0080	2.0062	2.0029	6.2	5.8	35.4	5.2	1.5	
DOTAP/DOPE Liposomes									
5-DPC	2.0087	2.0058	2.0025	5.5	5.7	33	7.2	10	0.49
16-DPC	2.0087	2.0058	2.0025	5.5	5.7	33	6.7	1	0.03
5-DSA	2.0089	2.0060	2.0029	6.2	6.3	33	6.4	10	0.5
16-DSA	2.0093	2.0060	2.0024	5.9	6	32.5	5.0	1	0.03

[a] Accuracy: $g_{ii} = \pm 0.0003$; A_{xx}, $A_{yy} = \pm 0.2$ G, $A_{zz} = \pm 0.5$ G; $\tau_\perp = \pm 0.2 \times 10^{-10}$ s; $S_{20} = \pm 0.03$; $n = \tau_\perp/\tau_\parallel$. [b] Accuracy: $g_{ii} = \pm 0.0003$; A_{xx}, $A_{yy} = \pm 0.2$ G, $A_{zz} = \pm 0.5$ G; $\tau_\perp = \pm 0.2 \times 10^{-10}$ s; $S_{20} = \pm 0.03$; $n = \tau_\perp/\tau_\parallel$.

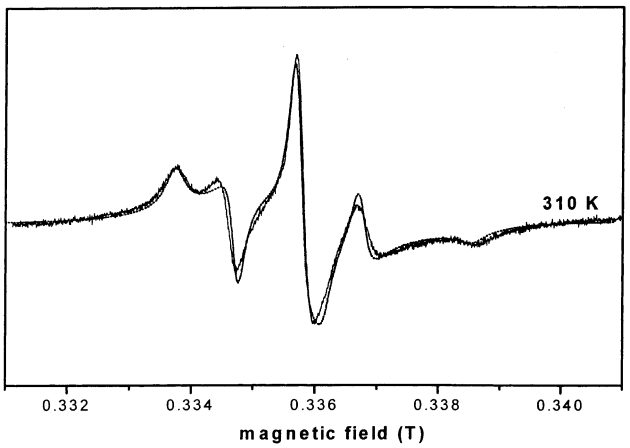

Figure 1. Experimental (full line) and calculated (dotted line) ESR spectra of 5-DPC 5×10^{-4} mol/dm^3 in the DOTAP/DOPE 1/1 (w/w) liposome water dispersion. Registration temperature: 310 K.

DOTAP/DOPE Liposomes Containing 5-DPC. Figure 1 shows the experimental and calculated ESR spectra of 5-DPC 5×10^{-4} mol/dm^3 in a DOTAP/DOPE liposome dispersion at physiological temperature ($T = 310$ K). This was the typical absorption of nitroxide molecules in restricted motion conditions, where the components of **A** and **g** tensors were not completely averaged. This spectrum was reproduced by summing two absorptions due to species in a slow chemical exchange: (i) an

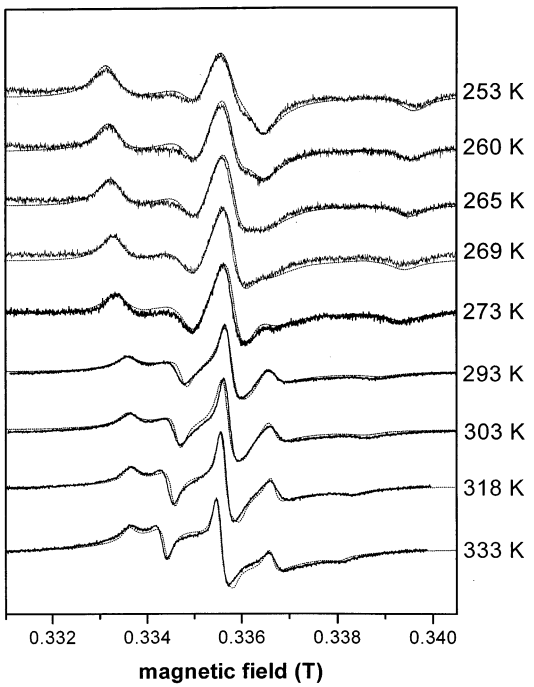

Figure 2. Experimental (full lines) and calculated (dotted lines) ESR spectra of 5×10^{-4} mol/dm^3 5-DPC in the DOTAP/DOPE 1/1 (w/w) liposome water dispersion. Registration temperature ranged from 253 to 333 K.

absorption in slow motion condition with the parameters reported in the Table 1 and (ii) the same absorption calculated with the same parameters given in Table 1, to which an additional line broadening arising from spin−spin effects in the slow-exchange limit ($\omega_{ex} = 2.5 \times 10^8$ s^{-1}) was added. This finding did not definitely establish the occurrence of two different spin probe populations that could be interpreted in the terms of two different concentrations of the spin probes in separate regions of the same liposome. The inclusion of the two components in the spectral calculation was then the only way we found to achieve a good fit to the experimental data. In different words, the MOMD model alone could not produce a satisfactory fit. Other inhomogeneous broadening mechanisms might also be able to account for the observed features in the experimental spectrum. However, segregation of PC-based nitroxides in bilayers is not uncommon, and it has been identified very recently either in the gel phase or in the liquid crystal phase.[26−28] Spin exchange phenomena also occur in single-component systems.[29,30] The above uncertainty did not alter the general conclusion arisen from the results reported in this paper (see below), which was based on the comparison of the ESR shapes from differently localized nitroxides and different temperatures. The conclusion was independent of spin exchange at all. An order parameter $S_{20} = 0.49 \pm 0.03$ characterized the 5-DPC spectrum.

Figure 2 shows the ESR spectra of the same system in the temperature range of 253−333 K. All of the spectra in Figure 2 were simulated with $\tau_\perp$ and $\tau_\parallel$ in the ranges 1.4×10^{-7}−4.3×10^{-10} s and 3.4×10^{-9}−4.3×10^{-11} s, respectively. The fact that $\tau_\parallel < \tau_\perp$ fully agreed with past and very recent literature on liposomes and membranes.[28,31,32] The 5-DPC probe sensed rapid motion conditions along its molecular axis, whereas reorientation in the plane perpendicular to this direction (expressed by $\tau_\perp$) occurred with longer times. In most of the tables and figures, reference was made to $\tau_\perp$, which is considered the most relevant of the two components, because it is strictly

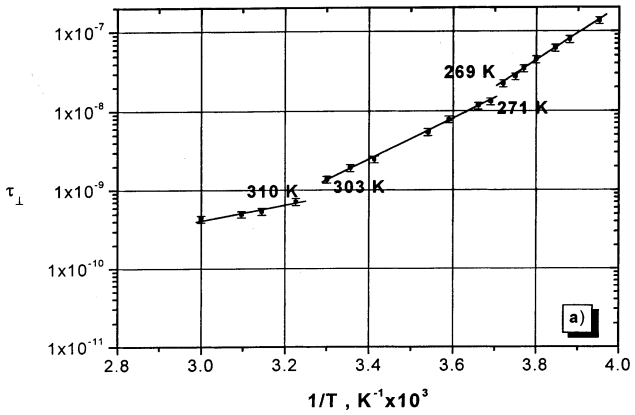

Figure 3. Correlation time $\tau_\perp$ of 5-DPC as a function of reciprocal temperature in the DOTAP/DOPE 1/1 (w/w) liposome water dispersion.

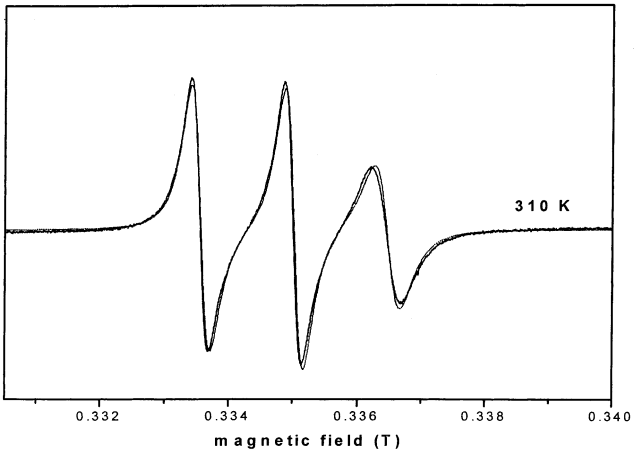

Figure 4. Experimental (full line) and calculated (dotted line) ESR spectrum of 16-DPC 5×10^{-4} mol/dm^3 in the DOTAP/DOPE 1/1 (w/w) liposome water dispersion. Registration temperature: 310 K.

correlated with the rotational wagging motion of the acyl chain long axis. With the increase of temperature from 253 to 333 K, the anisotropy of the diffusional motion, represented by $n = \tau_\perp/\tau_\parallel$, decreased from 40 to 10, and the order parameters S_{20} decreased from 0.85 to 0.40. Interestingly, from the temperature dependence of $\tau_\perp$ (Figure 3), two discontinuities of the correlation time appeared at $T = 269$−271 and 303−310 K. The same discontinuities were observed in the temperature dependence of $\tau_\parallel$. The order parameter ranged from 0.85 to 0.40 in the same temperature range. A clear discontinuity was observed at T = 267−269 K.

DOTAP/DOPE Liposomes Containing 16-DPC. Figure 4 shows the experimental (full line) and calculated (dotted line) 310 K ESR spectra of 5×10^{-4} mol/dm^3 16-DPC in DOTAP/DOPE liposomes. A quasirapid, isotropic motion characterized the spectral shape (Table 1). The paramagnetic unit in 16-DPC was located toward the middle of the bilayer where the order was very low (S_{20} near to 0). This region was an unpolar ($\langle A_N \rangle = 1.47$ mT) region, with a motion less hindered than in the environment sensed by 5-DPC. No anisotropy parameter was indeed introduced for spectral fitting, and just a small exchange frequency ($\omega_{ex} = 4.5 \times 10^7$ s^{-1}) was added to improve the agreement between calculated and experimental spectra.

Figure 5 shows the 16-DPC ESR spectra in DOTAP/DOPE liposomes in the temperature range of 261−333 K. Table 2 reports representative best-fit motional parameters. The same trend with temperature of $\tau_\perp$, $\tau_\parallel$, and S_{20} which was observed with 5-DPC, resulted from the 16-DPC spectral analysis as a

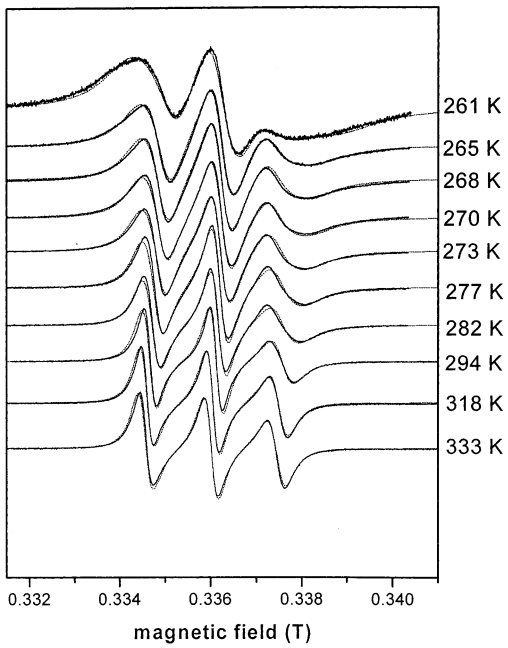

Figure 5. Experimental (full lines) and calculated (dotted lines) ESR spectra of 5×10^{-4} mol/dm^3 16-DPC in the DOTAP/DOPE 1/1 (w/w) liposome water dispersion in the temperature range of 253−333 K.

TABLE 2: Best-Fit Magnetic Parameters Which Accurately Reproduced ESR Spectra of 16-DPC in DOTAP/DOPE Liposomes at Different Temperatures[a]

T, K	n	$\tau_\perp$, s $\times 10^9$	S_{20}	ω_{ex}, Hz $\times 10^{-8}$
261	1	2.1	0.42	3
263	1	2.0	0.33	3
265	1	1.67	0.27	3
268	1	1.5	0.23	3
270	1	1.5	0.22	3
273	1	1.4	0.20	3
277	1	1.3	0.15	0.7
282	1	1.2	0.12	0.2
294	1	1.0	0.04	0.25
310	1	0.64	0.02	0.4
318	1	0.5	0.016	0.47
333	1	0.4	0.01	0.57

[a] Accuracy as in Table 1.

function of temperature. As with 5-DPC (Figure 3), marked discontinuities of the correlation times and of S_{20} were observed with 16-DPC at 265−268 K, which is almost at the same temperature reported for 5-DPC. The second discontinuity at about 293 K paralleled that one observed at 303−310 K.

As for the rotational diffusion constant $R_\perp$, it is worthy to note that the value we found in spectral simulation of 16-DPC in DOTAP/DOPE liposomes was of the same order of magnitude as those reported in the literature for similar systems. As an example, Ge and Freed[28] calculated $R_\perp = 1.08 \times 10^8$ s^{-1} for 16-DPC in DPPC bilayers. This value could be reasonably considered in line with the one we found for 16-DPC ($R_\perp = 2.5 \times 10^8$ s^{-1}): the discrepancy might be fully explained by the fact that palmitoyl chains are still in the gel state at 310 K, whereas the intrinsically more fluid oleoyl chains are in the liquid crystal phase.[33]

DOTAP/DOPE Liposomes Containing *n*-DSA. Although 5- and 16-DSA are nitroxides structurally different from *n*-DPC, they behaved almost in the same way in DOTAP/DOPE liposomes. ESR spectra of 5- and 16-DSA introduced into liposomes bilayers showed the same temperature trend as the corresponding *n*-DPC, with discontinuities of $\tau_\perp$, $\tau_{||}$, and S_{20} at

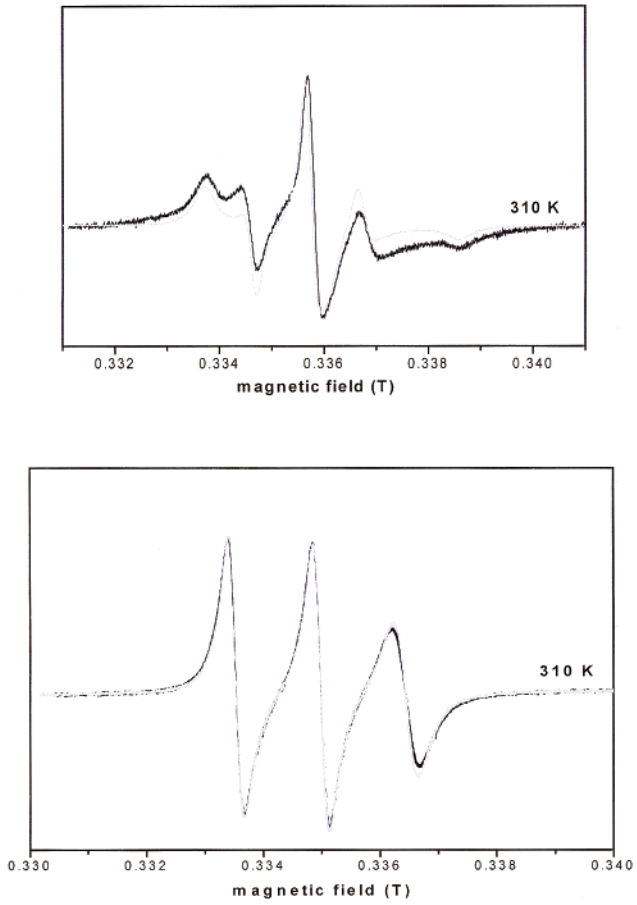

Figure 6. Top: ESR spectra of 5-DPC (full line) and of 5-DSA (dotted line) inserted into the same DOTAP/DOPE liposome dispersion (T = 310 K). Bottom: ESR spectra of 16-DPC (full line) and of 16-DSA (dotted line) inserted into the same DOTAP/DOPE liposome dispersion (T = 310 K).

almost the same temperatures found with *n*-DPC. Figure 6 shows superimposed ESR spectra of 5-DPC/5-DSA and 16-DPC/16-DSA inserted into DOTAP/DOPE liposomes with the same features, recorded in the same conditions. The best-fit magnetic parameters used for spectral simulation are compared in the Table 1. Faster reorientational rates were used for *n*-DSA than for *n*-DPC, and this was consistent with their smaller size and single hydrocarbon chain. An anisotropy ($n \geq 5$) was necessary to calculate the *n*-DSA spectra at temperatures lower than 265−270 K. A weak exchange frequency (ω_{ex} in the range of 10^6−10^8 s^{-1}) was also necessary. The values of the exchange frequency depended on the nitroxide concentration. When 16-DSA concentration of 10^{-4} mol/dm^3 or lower were used, the exchange frequency decreased up to vanish, although all other singularities of the ESR patterns did not change. This happened with each of the nitroxides used in this work.

Table 3 reports the activation energies for the spin probes in the different motional domains of the DOTAP/DOPE liposomes, as calculated from the correlation time trends with temperature. The ΔE_a values of 5-DPC were calculated from Figure 3, and the values of the other nitroxides were calculated from similar figures not reported in the text. The activation energies were of the correct order of magnitude for gel → liquid crystal (G → LC) and liquid crystal → liquid (LC → L) phase transitions in microscopically ordered systems. The ΔE_a values in the ordered gel phase of 5-DSA and 5-DPC, higher than those of 16-DSA and 16-DPC, once more agreed with the different motional properties of the bilayer regions sensed by the two types of

TABLE 3: Activation Energies (kJ/mol) for the Motion of *n*-DPC and *n*-DSA in the Different Phases of the DOTAP/DOPE Liposomes Containing Spin Probes

	gel[a]	liquid crystal[a]	liquid
5-DPC	29.1 ± 0.6−28.6 ± 0.6	21± 0.5−17.2 ± 0.4	7.9 ± 1.4−7.9 ± 1.4
5-DSA	38 ± 2−25 ± 2	11.0 ± 0.5−6.0 ± 0.6	3.0 ± 0.6−3.0 ± 0.6
16-DPC	5.4 ± 0.1	6.5 ± 0.4	6.5 ± 0.4
16-DSA	6.1 ± 0.4	7.2 ± 0.3	7.2 ± 0.3

[a] Values at left and at right refer to motion perpendicular ($\tau_\perp$) and parallel ($\tau_\parallel$) to the liposome bilayer. In the cases of 16-DSA and 16-DPC, only mean values are shown.

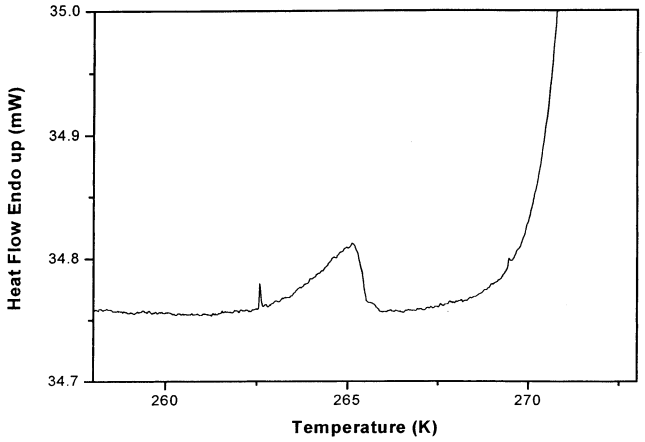

Figure 7. Enlarged endothermic DSC peak in the region of 258−273 K of DOTAP/DOPE 1/1 (w/w) liposome dispersion in water (total lipid concentration, 1%).

TABLE 4: Thermodynamic Data Obtained from DSC Runs of the Liposome Systems Investigated

system	ΔH_{peak} (kJ/mol of PL)	T_{max} (K)
pure liposome	28 ± 3	264 ± 2
liposome+ 5-DPC (10^{-3} mol/dm^3)	21 ± 2	263 ± 2
liposome + 5-DPC (5×10^{-4} mol/dm^3)	19 ± 2	263 ± 2
liposome +16-DPC (10^{-3} mol/dm^3)	23 ± 2	263 ± 2
liposome + 16-DPC (5×10^{-4} mol/dm^3)	14 ± 2	263 ± 2
liposome + 5-DSA (10^{-3} mol/dm^3)	22 ± 3	263 ± 2
liposome + 5-DSA (5×10^{-4} mol/dm^3)	16 ± 2	263 ± 1
liposome + 16-DSA (10^{-3} mol/dm^3)	25 ± 3	263 ± 2
liposome + 16-DSA (5×10^{-4} mol/dm^3)	19 ± 3	264 ± 3

radicals. The fact that the activation energies sensed by 5-DSA, 5-DPC, 16-DSA, and 16-DSA were roughly of the same order of magnitude of the activation energy of the viscous process of liquid water was a further proof of the molecular sensitivity of the ESR approach.

Differential Scanning Calorimetry. An intense peak was observed at $T = 273$ K that was due to the solid−liquid-phase transition of water solvent. The marked discontinuity at 267−271 K observed via ESR spectroscopy corresponded to a weak peak that was due to an endothermic event in the DSC curve of the plain DOTAP/DOPE liposome dispersions (Figure 7). A careful analysis below 273 K revealed this weak peak occurring in the range $T_m = 262-264$ K, with $\Delta H_m = 28$ kJ/mol of phospholipid, This value was of the same order of magnitude as those of pure phospholipids, depending on the nature and structure of these compounds.[33]

The significant thermodynamic data of the liposome systems investigated in this work are reported in Table 4.

The addition of a 5×10^{-4} mol/dm^3 solution of 5-DPC did not significantly change the overall features of the DSC curve of DOTAP/DOPE liposomes. The differences in the thermodynamic parameters of 5-DPC containing liposomes and those of nitroxide-free liposomes were the same in the experimental limit errors. Runs with lower and higher nitroxide (up to 10^{-3} mol/dm^3) concentrations and with 5-DSA, 16-DPC, and 5- and 16-DSA gave the same results. The small differences between temperatures of discontinuities in ESR quantities ($T = 266-273$ K) and in DSC peak temperatures ($T = 262-264$ K) are more apparent than real, because the evaluation of the DSC peak could be affected, for instance, by the near presence of the strong endothermic peak due to solid−liquid transition of water solvent.

From the above data, it resulted that, although ESR spectra clearly suggested that the nitroxides were imbedded in the liposome lipid bilayer, thermal data such as T_m and ΔH_m were not affected by the presence of the spin probe. This is an important finding that renders ESR spectroscopy of exogenous probes imbedded into liposomes a very reliable tool for the study of the dynamic properties without perturbing the physical status of the samples.

The discontinuity observed at $T \approx 300$ K deserves additional comments. No evidence of enthalpic changes was given in the DSC curves, which suggested that only a structural rearrangement of the molecules occurred. The same conclusion is reached by Tanaka and Freed,[31] who observe a phase transition 40−50 K above T_m of pure DPPC and DMPC bilayers and attribute this effect to an orientational rearrangement of the hydrocarbon chains, according to the Kimura and Nakano theory,[34] which predicts a strong change of the molecular packing together with a less pronounced change of the motional parameters, perfectly in line with the results reported in this work.

Conclusion

The combined use of ESR and DSC allowed us to obtain detailed information on the dynamics of cationic DOTAP/DOPE liposomes.

DSC thermograms showed weak endothermic peaks due to G → LC transitions. Neither transition temperatures T_m nor transition enthalpies ΔH_m depended appreciably on the presence of relatively concentrated exogenous molecules as the *n*-DSA and *n*-DPC spin probes are. This finding suggested a substantial invariance of the physical and structural properties of the liposome themselves after small loading.

The ESR spectra of the above spin probes confirmed, at a molecular level, the macroscopic results obtained with DSC. The spin probes localized inside the liposome bilayer and sensed different regions depending on the structure of the probe. From spectral simulation, discontinuities in the values of the relevant parameters for the motion and in the order parameter were found at $T = 266-273$ K, i.e., in a temperature range similar to that of the weak DSC peaks. A further discontinuity in the motional and order parameters, not observed in DSC patterns, resulted from the ESR calculation at temperatures in the range of 298−310 K, which was simply attributed to a molecular rearrangement of the lipid hydrocarbon chains. The S_{20} and $\tau_\perp$ discontinuities were less marked with 16-DSA and 16-DPC than with 5-DSA and 5-DPC: this was consistent with a smaller activation energy in the more mobile region toward the middle of the liposome bilayer. An explanation for the spin−spin effects, which led to line broadening, was given in terms of molecular motion, higher in the middle of the bilayer than near the surface of the liposome itself.

The marked anisotropy of the diffusion coefficient below T_m, as it arose from the high correlation time anisotropy $n = \tau_\perp/\tau_\parallel$,

proved that the environment sensed by 5-DPC and 5-DSA in liposomes was more ordered near the surface than toward the center of the bilayer.

The results shown here represent therefore an useful basis for the characterization of both plain and loaded liposomes aggregates suspended in aqueous environment, and they will be very useful when these liposomes are used as drug carriers.

Acknowledgment. The authors are in debt to University of Florence and Consorzio per lo Sviluppo dei Sistemi a Grande Interfase, CSGI, Italy, for financial and instrumental support. They also thank Dr. M. Mauro for his help in DCS measurements.

References and Notes

(1) Lasic, D. D. *Am. Sci.* **1992**, *80*, 20.
(2) Lasic, D. D. *Liposomes: From Physics to Applications*; Elsevier: Amsterdam, 1993.
(3) Rosoff, M., Ed.; Vesicles. In *Surfactant Science*; Ser. Dekker: New York, 1966; Vol. 62.
(4) Gregoriadis, G. *Elsevier Trends J.* **1995**, *13*, 527.
(5) Gregoriadis, G. *New England J. Med.* **1976**, *295*, 704; **1976**, *295*, 765.
(6) Wassan, K. M. Lopez-Berestein, G. *Immunopharmacol. Immunotoxicol*. **1995**, *17*, 1.
(7) Ristori, S.; Martini, G.; Schlick, S. *Adv. Colloid Interface Sci.* **1995**, *57*, 65.
(8) Martini, G.; Ristori, S.; Visca, M. In *Physical Chemistry of Ionomers*; Schlick, S., Ed.; CRC Press: Boca Raton, FL, 1996; Chapter 10, pp 219−250.
(9) Rossi, S.; Ristori, S.; Pozzi, L.; Martini, G. *Inorg. Chim. Acta* **1998**, *272*, 274.
(10) Ristori, S.; Rossi, S.; Ricciardi, G.; Martini, G. *J. Phys. Chem. B* **1997**, *101*, 8507.
(11) Rossi, S.; Karlsson, G.; Ristori, S.; Martini, G.; Edwards, K. *Langmuir* **2001**, *17*, 2340.
(12) Ristori, S.; Maggiulli, C.; Appell, J.; Marchionni, G.; Martini, G. *J. Phys. Chem. B* **1997**, *101*, 4156.
(13) To be published.
(14) Gruner, S. M.; Tate, M. W.; Kirk, G. L.; So, P. T. C.; Turner, D. T.; Keane, D. T.; Tilcock, C. P. S.; Cullis, P. R. *Biochemistry* **1988**, *27*, 2853.
(15) Zvidam, N. J.; Barenholz, Y. *Biochim. Biophys. Acta* **1997**, *1329*, 211.
(16) Guarini, G. G. T.; Dei, L. *Thermochim. Acta* **1995**, *250*, 85.
(17) Schneider, D. J.; Freed, J. H. *Biological Magnetic Resonance. Spin Labeling. Theory and Applications*; Berliner, L. J., Reuben, J., Eds.; Plenum Press: New York, 1989; Vol. 8, p 1 and references therein.
(18) Budil, D. E.; Lee, S.; Saxena, S., Freed, J. H. *J. Magn. Reson.* **1996**, *120*, 155.
(19) Meirovitch, E.; Nayeem, A.; Freed, J. H. *J. Phys. Chem.* **1984**, *48*, 3454.
(20) Ge, M.; Freed, J. H. *Biophys. J.* **1998**, *74*, 910.
(21) Benatti, C. R.; Feitosa, E.; Fernandez, R. M.; Lamy-Freund, T. M. *Chem. Phys. Lipids* **2001**, *111*, 93.
(22) Berliner, L. J., Ed.; *Biological Magnetic Resonance. Spin Labeling: The Next Millennium*; Plenum Press: New York, 1998; Vol. 14.
(23) Butterfield, D. A. In *Biological Magnetic Resonance*; Berliner, L. J., Reuben, J., Eds.; Plenum Press: New York, 1982; Vol. 4, p 1.
(24) Hemminga, M. *Chem. Phys. Lipids* **1983**, *32*, 323.
(25) Berliner, L. J., Ed.; *Spin Labeling. Theory and Applications*, Academic Press: New York, 1976 (1979); Vols. 1 and 2.
(26) Veiga, M. P.; Goñi, F. M.; Alonso, A.; Marsh, D. *Biochemistry* **2000**, *39*, 9876.
(27) Veiga, M. P.; Arrondo, J. L.; Goñi, F. M.; Alonso, A.; Marsh, D. *Biochemistry* **2001**, *40*, 2614.
(28) Ge, M.; Freed, J. H. *Biophys. J.* **1999**, *76*, 264.
(29) Earle, K. A.; Moscicki, J. K.; Ge, M.; Budil, D. E.; Freed, J. H. *Biophys. J.* **1994**, *66*, 1213.
(30) Fajer, P.; Watts, A.; Marsh, D. *Biophys. J.* **1992**, *61*, 879.
(31) Tanaka, H.; Freed, J. H. *J. Phys. Chem.* **1984**, *88*, 6633.
(32) Jingyan, Z.; Luz, Z.; Zimmerman, H.; Goldfarb, D. *J. Phys. Chem. B* **2000**, *104*, 279.
(33) Cevc, G. *Phospholipids Handbook*; Dekker: New York, 1993.
(34) Kimura, H.; Nakano, H. *Mol. Cryst. Liq. Cryst.* **1981**, *68*, 289.